

Development of a mobile robot-based combined sensor platform to determine the correlation between soil penetration resistance and electrical conductivity

İlker ÜNAL^{1,*}, Mehmet TOPAKCI², Murad ÇANAKCI², Davut KARAYEL², Erdem YILMAZ³, Önder KABAŞ⁴

¹Department of Mechatronics, Technical Science Vocational School, Akdeniz University, Antalya, Turkey

²Department of Agricultural Machinery and Technologies Engineering, Faculty of Agriculture, Akdeniz University, Antalya, Turkey

³Department of Soil Science and Plant Nutrition, Faculty of Agriculture, Akdeniz University, Antalya, Turkey

⁴Department of Machine, Technical Science Vocational School, Akdeniz University, Antalya, Turkey

Received: 14.07.2020 • Accepted/Published Online: 08.05.2021 • Final Version: 23.06.2021

Abstract: Open-field farming involves successive major processes such as preparation of soil, planting the seed, adding pesticides and fertilizers, irrigation, cultivation, and harvest. The main aim of all processes is to achieve maximum yield out of the available agricultural landscape. It is necessary to collect geo-referenced descriptive data on soil characteristics, such as soil penetration resistance and electrical conductivity before starting all these processes. In this context, agricultural robots offer highly promising technologies providing valuable soil data, lower production costs, reduced manual labour, and maximum crop efficiency. The aim of this study is to design and develop a combined sensor platform and a GPS-guided 4WD agricultural autonomous robot to provide rapid measurement and mapping of the soil penetration resistance and the electrical conductivity for precision farming applications. The agricultural robot is a nonholonomic mobile robot, which has a differential steering mechanism and can be forwarded to stable-target points. The combined sensor platform, which is a y-axis shifter driven by a DC motor with reducer, consists of the Wenner array probes and load cell-based penetration rod. AutoCAD software was used for designing and drawing of the robot and measurement platform. All software was coded in Microsoft Visual Basic.NET programming language. Field studies were conducted to measure the soil penetration resistance, electrical conductivity, and determine the correlation between soil penetration resistance and electrical conductivity. As a result, the ranges of the soil measurement were observed between 1.13 MPa-2.14 MPa for penetration resistance and 0.14–0.33 dS/m for electrical conductivity. Results showed that there is a fairly strong negative relationship between the soil penetration resistance and the electrical conductivity ($R^2 = -0.78$).

Key words: Combined sensor platform, agricultural robots, soil penetration resistance, soil electrical conductivity, precision farming, mapping

1. Introduction

Soil penetration resistance and electrical conductivity are important physical indicators affecting the plant root growth. The penetration resistance that is often used as a surrogate measurement correlates with the energy requirements of tillage implements, vehicle trafficability, and plant root growth (Alesso et al., 2019). The penetration resistance, which can change with soil spatial variability, variable weather conditions, and implementation of varying soil and crop management practices, must be evaluated together with water content and soil type (Lima et al., 2017). Penetration resistance and water content are inversely proportional because of the fact that when the penetration resistance increases, water content decreases (Siqueira et al., 2014).

The soil compaction, which is highly influenced by the soil water content, is a serious problem causing to alter soil structure, limits water and air infiltration, and reduces root penetration in the soil (Nawaz et al., 2013). Also, the soil water content affects the penetration resistance. If a soil has low soil water content, the soil is less vulnerable to compaction. But when the soil has high water content, the soil becomes less compressible. Ishaq et al. (2001) showed that the soil compaction is sensitive to the amount of water content and when the water content in the soil increases up to a limit, soil compaction decreases with the increasing water contents. Also, Barnhisel (1997) presented the interrelationship among components of water content, soil compaction, and yield. On the other

* Correspondence: ilkerunal@akdeniz.edu.tr

hand, the highest penetration resistance causes the lowest yields, and the lowest penetration resistance causes the highest yields (Servadio et al., 2016).

The penetrometer, which is a rod with a certain diameter conical tip that is forced vertically into the soil by the operator's hand force or an electromechanical motor, is an extremely simple device used for measuring the soil penetration resistance. Soil penetration resistance, which is known as cone index (CI), is calculated by dividing the force needed to insert the rod into the soil at a constant rate of penetration by the base area of the cone. The penetration resistance is a function of rod size, shape, size of cone tip, and rate of penetration as well as soil type, density, and moisture conditions (Valera et al, 2012). The constant penetration speed that is an important criterion to make accurate measurements can provide by using direct current (DC) motor to perform the penetration.

Soil moisture is a feature that has both spatial and temporal variability in the field. In field measurements, soil moisture and penetration measurements generally cannot be taken at the same spatial location. In order to better interpret the penetration resistance data, it is necessary to measure both penetration resistance and soil moisture from the same spatial location. According to the requirement of practicality and accuracy, there are a few methods of measuring soil moisture from the simplest to advanced technology, such as appearance and feel method, tensiometer, gypsum block, neutron probe meter, gravimetric method, time-domain reflectometry (TDR) probe, thermal conductivity, optical method, dielectric method, and the Wenner method. Measurement results are influenced by factors such as soil type, factory calibration of the device, inadequate device-soil contact, temperature, and electrical conductivity. For this reason, improper measurements can lead to wrong interpretation of the measured readings. However, the Wenner method, which consists of measuring the soil conductivity using four probes, stands out for automation capability, real-time measurements, easy setup configuration, and measuring for different soil depth. In this method, soil salinity is an important factor to measure the water content. The Wenner four-probe method provides valuable electrical conductivity data in determining the composition of soil, for example, as water content, moisture, salinity, porosity, organic matter level, bulk density, and soil texture.

Today, a lot of agricultural activities are being done by using smart farming technologies such as Internet of Things, artificial intelligence, machine learning, and precision farming. These technologies are used for crop and soil monitoring, predictive analysis, agricultural robotics, and variable rate technology. One of the top trends driving agriculture in recent years is precision farming based variable rate technology, which uses

different technologies to make farming more efficient and sustainable, offering the potential of higher yields with less labour while using less soil, water, and chemicals. Also, data collection, especially soil penetration resistance and electrical conductivity, and its interpretation is an important data source for variable rate applications and should be done comprehensively and intensively. Data collection on the field is highly dependent of temporal and spatial variations, which require higher data acquisition frequency and precision. Traditional data collection consists of manually probing the soil and collecting the samples into the container to analyze at the laboratory. If we want to collect more soil samples, this method is tedious and time-consuming (Valjaots et al., 2018). On the other hand, it is clear that the agricultural robotics assists with new methods of real-time data collection for more innovation. The future of agriculture is becoming more sophisticated, and the agricultural robot usage is expected to increase by 24.1% until 2024. And also, the agricultural robots market is expected to reach \$11.58 billion by 2025 according to verified market researches (VMR, 2018). Agricultural robots can be used for weeding, harvesting, spraying, environmental monitoring, and soil analysis.

The soil is under the influence of the various physical parameters, which can affect each other and all can directly reduce soil quality (Feng et al., 2019). In previous studies for the instantaneous measure of physical soil parameters, researchers are generally focused on the measurement of a single parameter (Naderi-Boldaji et al., 2011). However, the measurement of a single parameter does not provide sufficient information to evaluate the general structure of the soil, and, thus, it is necessary to measure more than one parameter using multisensor techniques (Zeng et al., 2008). The objective of this study was to design and develop a 4WD Agricultural Robot and combined sensor platform for the simultaneous on-the-go measurement of soil penetration resistance and electrical conductivity. And also, the linear and spatial correlation between soil resistance penetration and apparent soil electrical conductivity was determined in this study.

2. Materials and methods

The subject of the study is to develop, design, and implement a prototype of a 4WD Agricultural Robot with a combined sensor platform to measure the soil penetration resistance and soil electrical conductivity. The main goal of the project is to determine the correlation between soil penetration resistance and soil electrical conductivity. The study consists of three main sections:

1. 4WD autonomous mobile robot and steering algorithm: The mobile robot, which can be steered point-to-point autonomously, was equipped with a four-wheeled differential steering system with a nonholonomic

constraint structure. The combined sensor platform is attached to the mobile robot.

2. Combined sensor platform: It is attached to the 4WD mobile robot and it moves vertically to dip the penetration rod and the Wenner probes in the soil. The penetration rod and the Wenner probes are attached to the movable platform to measure the soil penetration resistance and electrical conductivity instantaneously.

3. Field data collection system, software developments and field trials: The system is used to collect data from DGPS receiver, digital compass, load-cell indicator, and digital multimeter on the measurement platform for the storing and mapping process. A program was developed to autonomously steer the mobile robot, to retrieve data from all electronic equipment, and to insert all data into the database.

2.1. 4WD autonomous mobile robot mechanical design and steering algorithm

Autonomous mobile robot generally can be steered from point to point in the agricultural field conditions by using a four-wheel differential steering mechanism with nonholonomic constraints structure. The full-scale technical drawing of the designed 4WD autonomous mobile robot is shown in Figure 1a. The figure of the produced autonomous robot, which has the combined sensor platform, is shown in Figure 1b.

The robot was powered by four 24 V - 0.25 kW - 1440 rpm brushed DC motors, which were coupled to the wheels through a gear mechanism, whose gear ratio is $i = \omega_M/\omega_L = 10$. All motors are mechanically independent, but the front and rear motors on both sides are electrically connected to each other's to provide differential steering. The wheels were chosen to be the rubber 2.50 × 17 motorcycle wheel and tube. Two rechargeable maintenance-free gel batteries wired in series (each one's capacity is 12V 72 Ah) were used for the operation of electronic components and motors. In addition, a 300 W DC/AC inverter was used to supply the industrial computer, electronic compass, and the GPS receiver. The total weight of the robot with all the components is about 150 kg, the width is about 1610 mm, and the body height is about 1230 mm. The gearbox output torque for each wheel was 17.05 Nm. A wheel has an outside diameter of 560 mm and the shaft speed was 140 rpm. The robot speed was 14.77 km/h. And also, the shaft torque was 32.93 Nm. The rolling resistance coefficient was used as 0.085. This value is suggested for off-road (unpaved surface) applications.

The RoboteQ's FDC3260 (RoboteQ Inc., Arizona, USA) three-channel motor controller was used to move and steer the designed mobile robot. The FDC3260 can accept operation commands received from a computer serially. The FDC3260 motor controller was connected to the industrial computer on the mobile robot via its

RS232 port. The electrical wiring diagram between the motor controller and DC motors, battery and industrial computer is shown in Figure 2.

When the controller connects to the industrial computer, communication is done without flow control, meaning that the controller is always ready to receive data and can send data at any time. The commands are sent to the motor controller via the developed navigation software. Waypoint that includes destination latitude and longitude value is the most important navigation data that helps the mobile robot knows where it is and where it is going. In this study, waypoints were inserted beforehand into the industrial computer database for the steering algorithm. On the other hand, heading and azimuth angles are the most significant and necessary data for the navigation of mobile robots. The heading angle is the angle between true North and the mobile robot's centerline in the horizontal plane measured in the clockwise direction. The Honeywell HMR3000 digital compass (Honeywell Inc., North Carolina, USA) was used to measure the heading angle of the mobile robot. The azimuth angle is the angle between true North and the target point in the horizontal plane measured in the clockwise direction. The Promark 500 GPS (Magellan Co., Santa Clara, CA, USA) receiver was used to acquire the geographical coordinates of the mobile robot.

2.2. Combined sensor platform

The developed combined sensor platform is shown in Figure 3. The measuring unit was mounted on a linear slide-guide system which moves vertically on an H-shaped carrier grid that has mounted to the mobile robot. It was used a 24 V - 500 W - 1440 rpm DC motor, which was coupled to a 1: 40 reduction gearbox for the vertical movement of the measuring unit. The measurement unit has one penetration rod and the four Wenner probes. The penetrometer rod is made of steel. The length of the penetration rod is 500 mm. The cone angle of the penetration rod is 30°. The cone point of the penetration rod has a base area of 634.20 mm² and a conical area of 1250.32 mm². The load cell was placed in the center of the measuring unit. Afterward, the penetration rod was fixed to the load cell. Four steel Wenner probes were linearly mounted on the measuring unit at 500 mm intervals to measure the electrical conductivity values of the soil between 0–500 mm. The fiber isolation rings were used to provide electrical isolation between the measuring unit and the Wenner probes. The Wenner probes' length is 25 mm and 12 mm in diameter. The probe length may not exceed 1/20 of the spacing of the Wenner array (Ünal et al., 2020). The C1 and C2 probes in the Wenner array were connected to a 24 V battery using the insulated single core cable to inject electric current into the soil. P1 and P2 probes were connected to the digital multimeter to

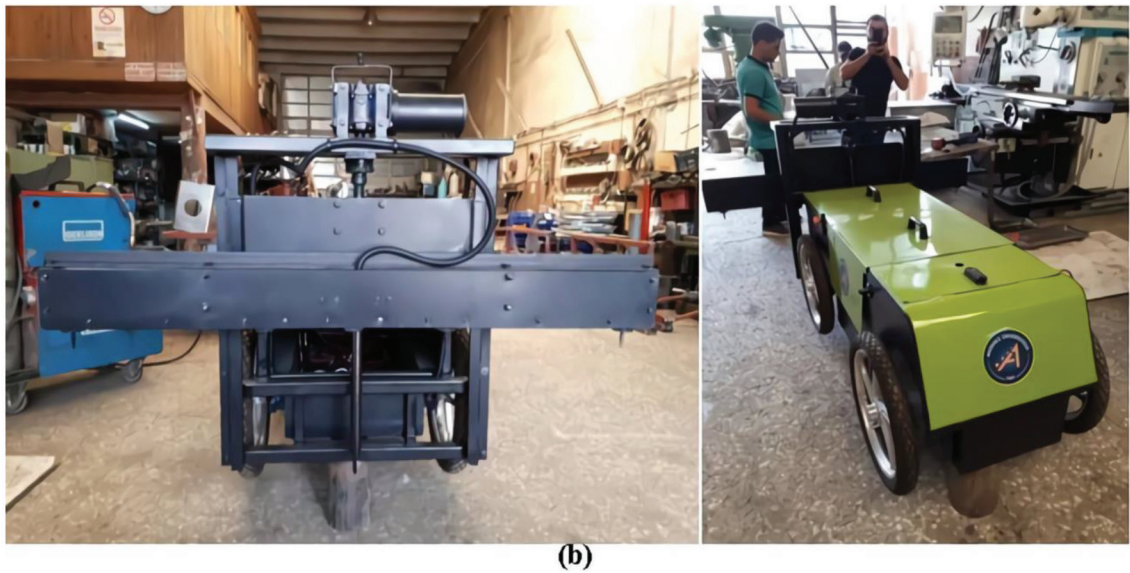
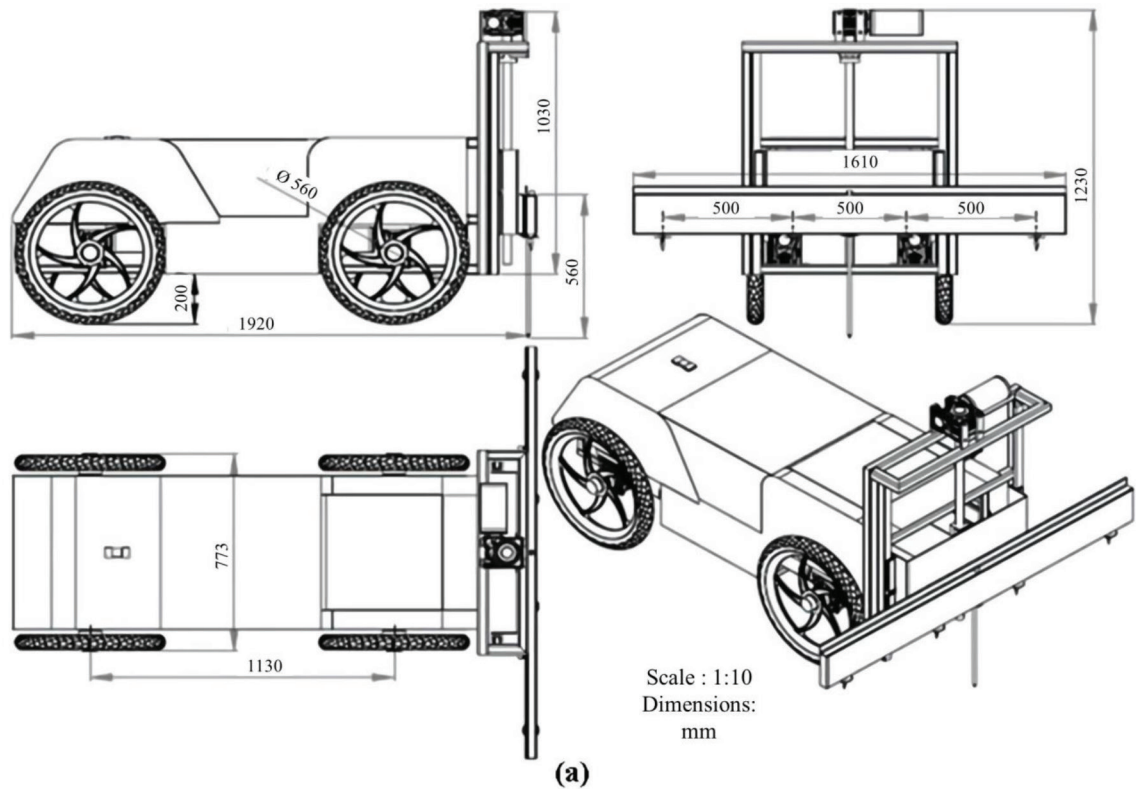


Figure 1. a) The full-scale technical drawing of the 4WD autonomous mobile robot. b) The figure of the produced autonomous robot.

measure the potential difference between probes caused by the electric current injected into the ground.

In this study, Wenner probe array was used to measure the apparent soil electrical conductivity (ECa). In Wenner probe array, the two outer probes, C1 and C2, are current

electrodes, and the two inner probes, P1 and P2, are potential electrodes (Figure 4). The Wenner based ECa measurement is calculated with Equation (1):

$$EC_a = 1 / (2 * \pi * a * R_w) \quad (1)$$

where: ECa is Siemens per meter (S/m), a is the probe

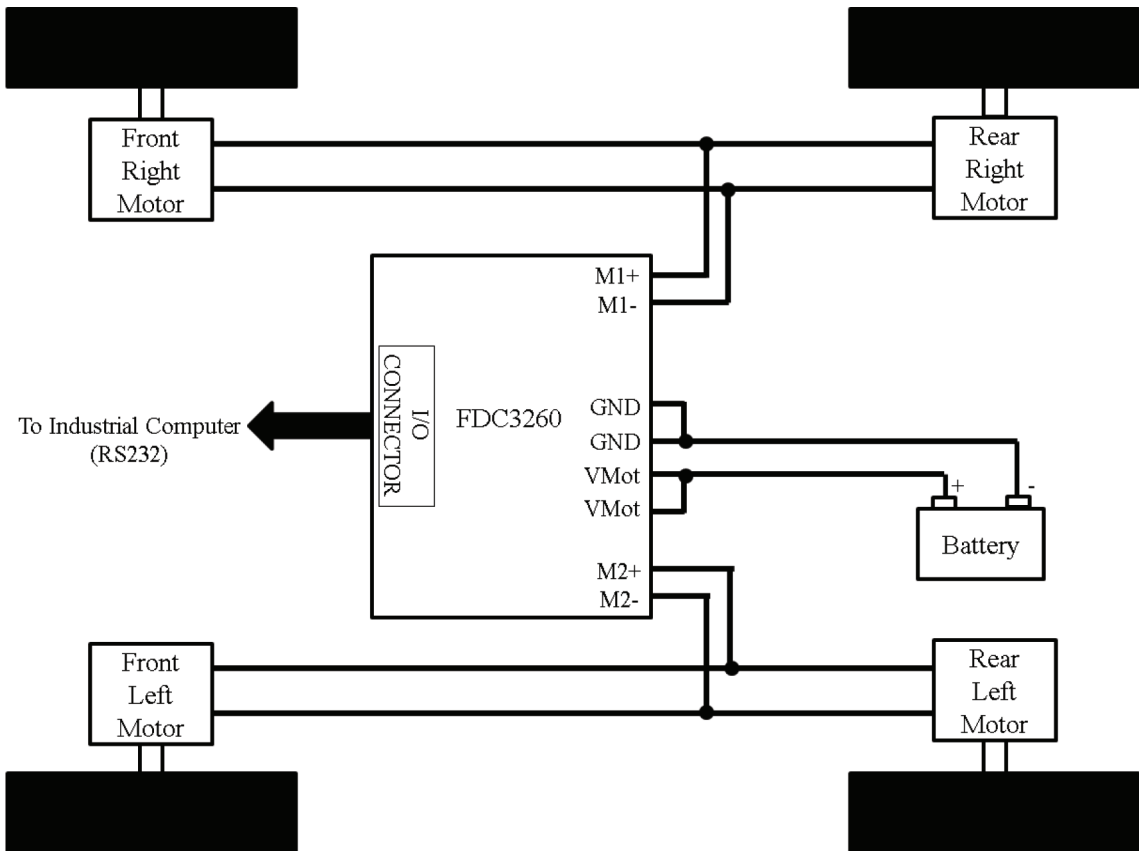


Figure 2. Mobile robot's electrical wiring diagram.

spacing (m), and R_w is the Wenner Resistance (ohm). R_w was measured with the Protek 506 digital multimeter (Hung Chang Co. Ltd., Seoul, KOR).

The S-type 500 kg capacity load cell (Zemic Europe B.V., Leerlooierstraat, NL) was used as a force transducer to measure the soil penetration resistance. The R320 indicator (Rinstrum Pty Ltd., Brisbane, AUS), which converts load cell outputs as weights, was used to send data to the industrial computer. The placement of the Wenner array, penetration rod, and the load cell is shown in Figure 5.

The soil penetration resistance, which is called the cone index (CI), was calculated by using the Equation (2). In this calculation, the penetration rod was immersed into the soil at a speed of 30 mm/s with the help of the DC motor.

$$CI \text{ (MPa)} = (F \text{ (N)}) / (A \text{ (mm}^2)) \quad (2)$$

In Equation 2, the F (Force) was calculated by multiplying the indicator value of the load-cell (Kg) by the earth's gravity (9.81 m/s²). The A (Area) is the base area of the penetration cone of the penetration rod.

2.3. Field data collection system, software developments, and field

In this study, the Lilliput 7" industrial-grade embedded platform, the PC-700 Panel PC system was used as the central computer because of the plethora of its communications interfaces. The PC-700 Panel PC has five COM ports for RS232 communication. All the electronic instruments were connected to the industrial computer through RS232 port. The GPS receiver was used to send raw GPS data based on NMEA 0183 (National Marine Electronics Association) protocol to the industrial computer for determining the position of the mobile robot and the location of the measured points. The NMEA sentence \$GPRMC was used to provide essential information, such as latitude and longitude coordinates. The Rinstrum R320 indicator was used to send weighing data using the ASCII-based communication syntax to the mobile robot's industrial computer. The HMR3000 digital compass was used to send heading, pitch, and roll outputs through simple ASCII character command strings (NMEA 0183) to the industrial computer for the mobile

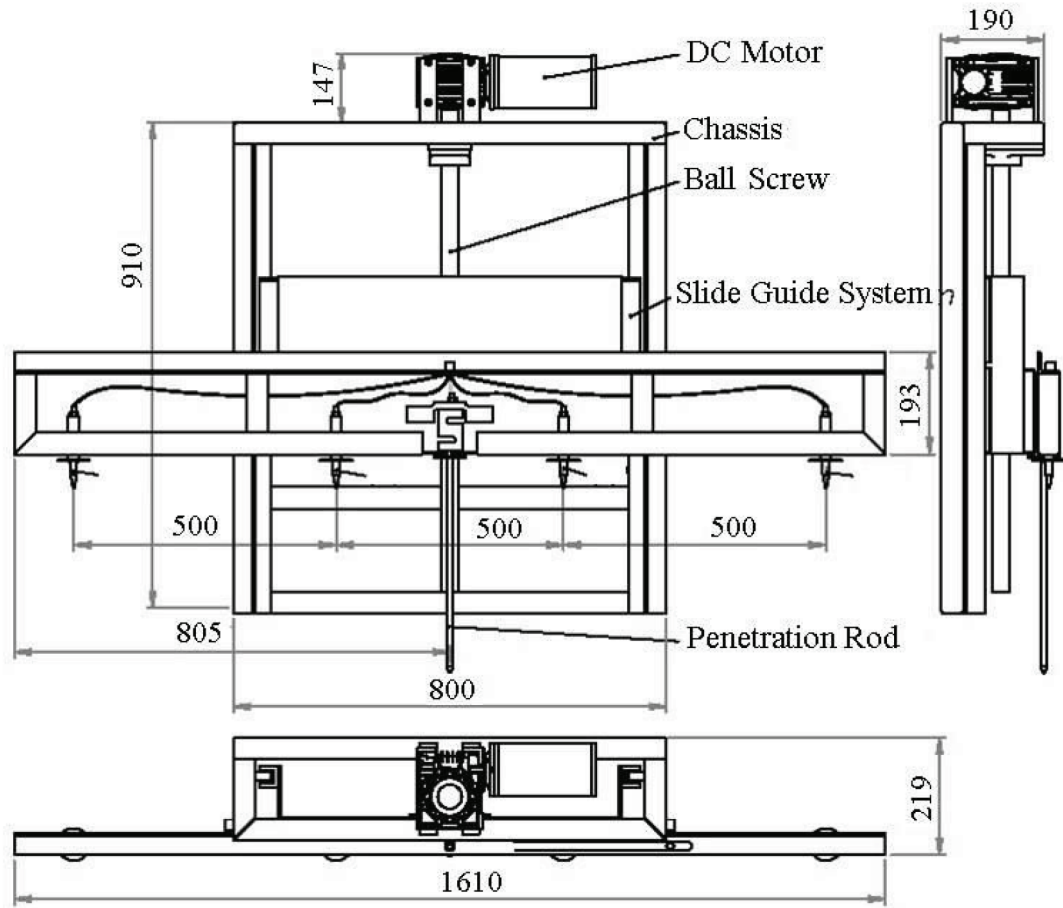


Figure 3. Full scale technical drawing of the combined sensor platform.

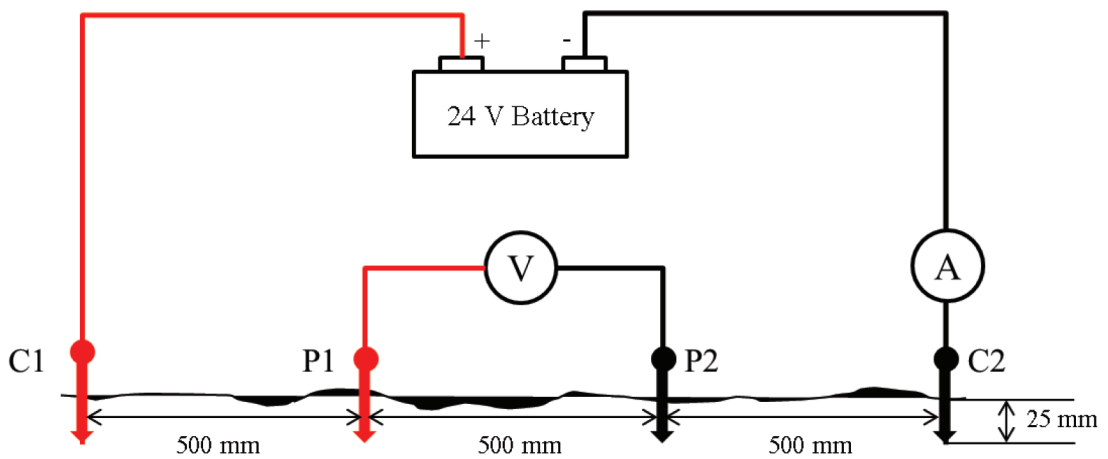


Figure 4. Wenner probe array configuration.

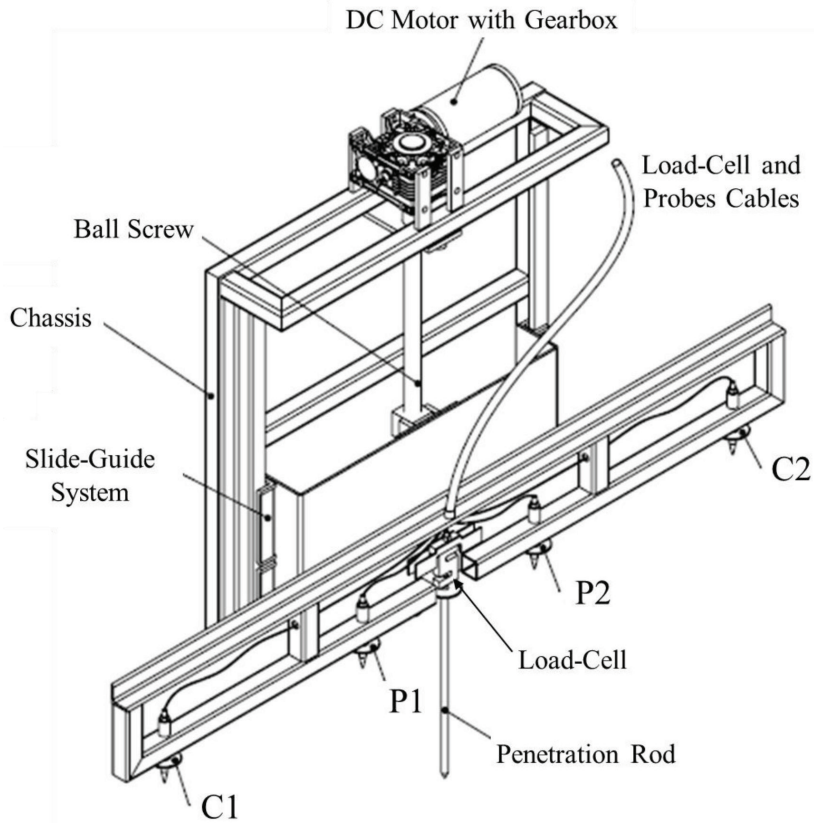


Figure 5. The placement of the Wenner array, penetration rod, and load cell.

robot navigation. The Protek 506 digital multimeter was used to measure and send the Wenner resistance and the voltage difference between P1 and P2 probes through simple ASCII character command strings to the industrial computer.

A program was coded using Microsoft Visual Basic.NET 2015 programming language to steer robot autonomously and control the measurement system (Figure 6). It was used to collect all data relevant to the spatial conditions during the field study, including GPS data, heading data, soil penetration resistance data, and soil electrical conductivity data. All data was instantly recorded in SQL Server 2005 database.

The field trials were conducted at the Batı Akdeniz Agricultural Research Institute, in Aksu, Antalya, Turkey (36°56'34.46" N and 30°53'04.10" E) to determine the correlation between the soil penetration resistance and the electrical conductivity. A test field has an area of 1.2 ha and an elevation of approximately 35 m above the sea level. The soil of the trial field has a silty-clay texture with 18% sand, 40% silt, and 42% clay. At the start of the experiment, the soil organic matter content was 1.4%. The test field was shown in Figure 7.

The mobile robot is capable of following a sequential list of waypoints entered by the user to find its way to the target point. For this reason, the 72 different waypoints of the mobile robot were stored into the application database at the start of the field trials. In the field trials, the robot, which uses the autonomous stop-and-go measurement method, was autonomously steered to 72 different waypoints, and the soil penetration resistance and the electrical conductivity values were collected for 0-50 cm depth.

3. Results

During the test within the 1.2 ha test field, the mobile robot was autonomously steered to 72 different geographical spots and soil penetration resistance and electrical conductivity values were collected for 0-50 cm depth (Table 1). The maximum and minimum values of the measured soil penetration resistance values were 1.13 and 2.14 MPa, respectively. Also, the maximum and minimum values of the measured soil electrical conductivity values were 0.14 and 0.33 dS/m, respectively. In this study, all measured data were stored into Microsoft SQL Server 2005 database and imported into ArcGIS 10.5 software for spatial

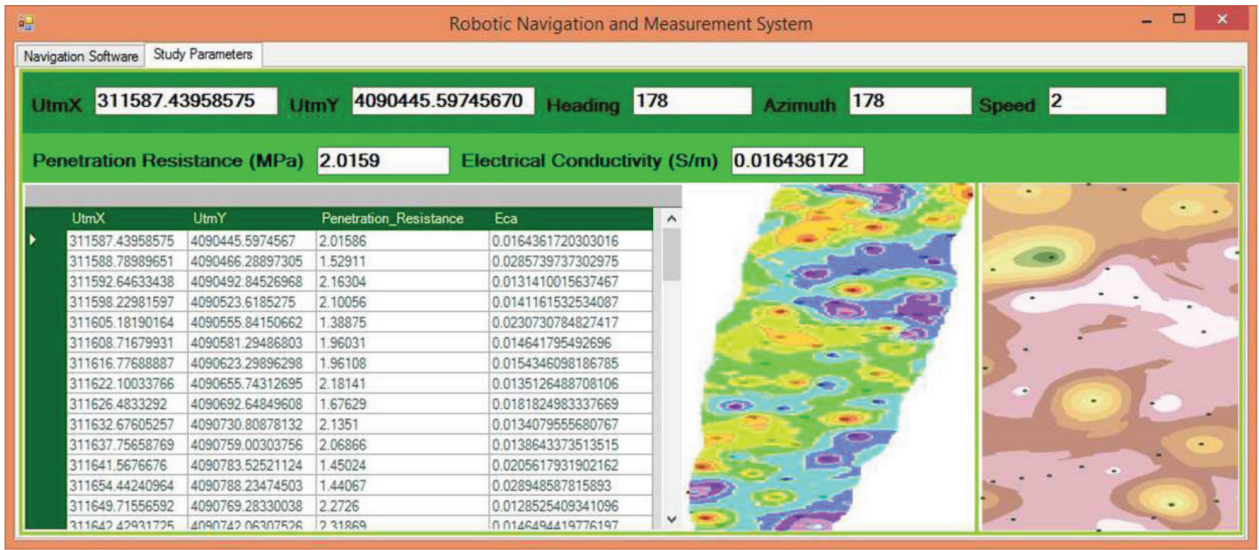


Figure 6. Study parameters for measurement system.

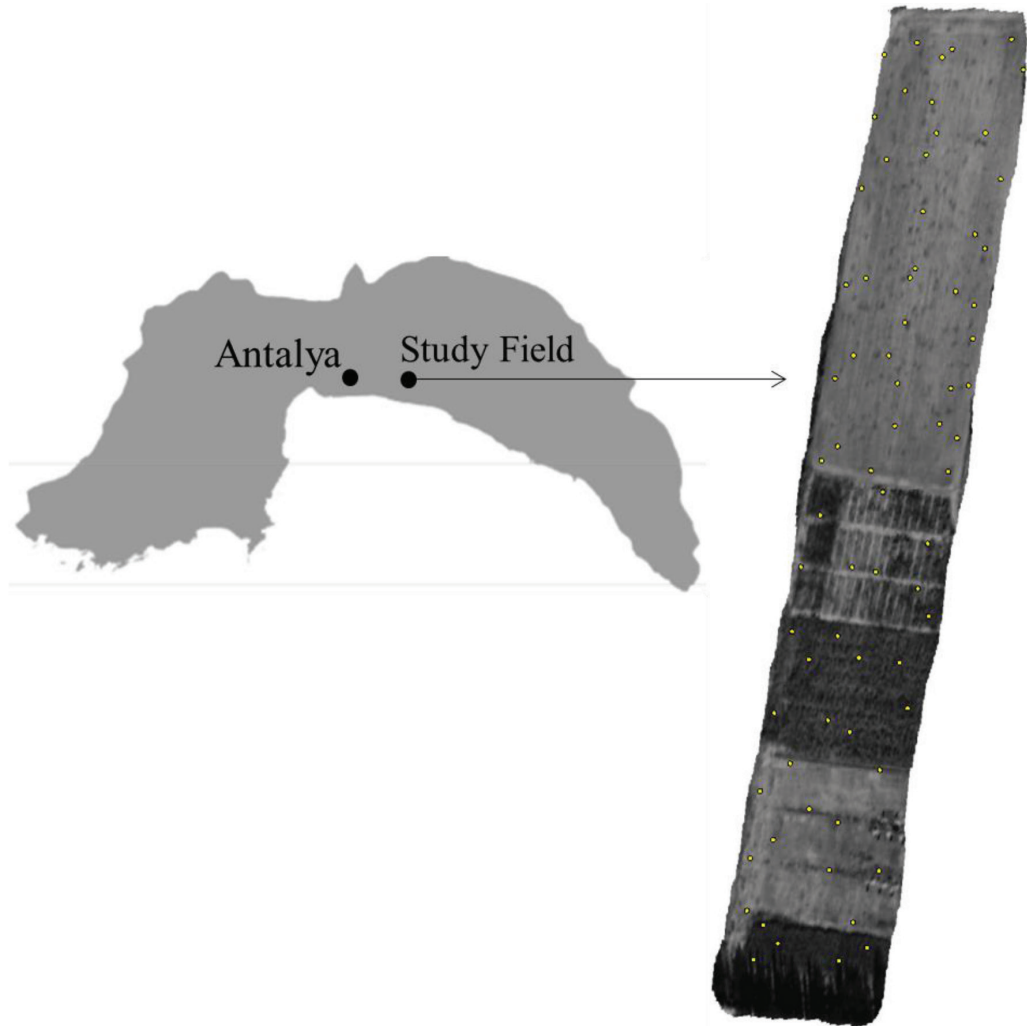


Figure 7. The test field.

Table 1. Geographical spots, soil penetration resistance, and electrical conductivity values.

No	UtmX	UtmY	PR (MPa)	ECa (dS/m)	No	UtmX	UtmY	PR (MPa)	ECa (dS/m)
1	311587.4396	4090445.5975	1.92	0.16	37	311662.1143	4090752.5419	1.94	0.16
2	311588.7899	4090466.2890	1.53	0.29	38	311656.6754	4090721.5803	1.59	0.23
3	311592.6463	4090492.8453	2.11	0.14	39	311653.6516	4090699.0758	1.61	0.21
4	311598.2298	4090523.6185	2.00	0.14	40	311649.6176	4090677.8889	2.03	0.14
5	311605.1819	4090555.8415	1.39	0.23	41	311646.7052	4090653.7168	1.31	0.27
6	311608.7168	4090581.2949	1.96	0.15	42	311645.5897	4090636.9053	2.02	0.15
7	311616.7769	4090623.2990	1.96	0.15	43	311640.8511	4090610.7386	1.53	0.20
8	311622.1003	4090655.7431	2.11	0.14	44	311638.0755	4090579.3479	1.64	0.21
9	311626.4833	4090692.6485	1.68	0.18	45	311631.5319	4090545.4508	1.79	0.16
10	311632.6761	4090730.8088	2.14	0.14	46	311627.9109	4090516.1140	1.87	0.15
11	311637.7566	4090759.0030	2.07	0.14	47	311623.2556	4090480.3248	1.54	0.19
12	311641.5677	4090783.5252	1.55	0.21	48	311619.8685	4090461.5286	1.71	0.14
13	311654.4424	4090788.2347	1.24	0.29	49	311663.2804	4090637.8077	2.05	0.14
14	311649.7156	4090769.2833	2.13	0.14	50	311669.6364	4090690.0254	2.06	0.16
15	311642.4293	4090742.0631	2.02	0.15	51	311681.2725	4090752.6716	2.01	0.14
16	311634.2627	4090695.2510	1.36	0.24	52	311667.7481	4090651.7695	1.61	0.20
17	311629.4297	4090664.8311	1.57	0.20	53	311658.6678	4090590.5467	1.59	0.14
18	311623.1378	4090628.8931	2.08	0.14	54	311654.7076	4090572.6883	1.64	0.16
19	311616.2966	4090601.6631	1.96	0.17	55	311647.5245	4090543.4306	2.11	0.14
20	311611.9156	4090544.7762	1.84	0.14	56	311623.6775	4090425.7365	1.39	0.23
21	311604.4696	4090503.6835	1.64	0.18	57	311629.2130	4090440.9697	1.45	0.23
22	311597.8636	4090473.6730	1.24	0.23	58	311639.7532	4090501.0501	1.40	0.23
23	311593.8430	4090439.7199	2.13	0.14	59	311666.7208	4090618.8600	1.96	0.14
24	311590.1296	4090426.2963	2.05	0.17	60	311677.2653	4090712.6127	1.58	0.20
25	311599.6239	4090432.5610	1.84	0.16	61	311691.5961	4090789.6302	1.67	0.14
26	311611.9420	4090485.7563	2.06	0.15	62	311696.2272	4090777.5015	2.12	0.14
27	311619.4009	4090520.7433	1.85	0.15	63	311687.2524	4090734.4076	1.62	0.21
28	311623.1081	4090553.9634	1.55	0.20	64	311681.1495	4090706.9761	1.63	0.21
29	311628.9103	4090581.2165	2.13	0.14	65	311676.7900	4090684.5012	2.02	0.14
30	311636.2904	4090619.3505	2.03	0.15	66	311676.3502	4090671.3750	1.35	0.26
31	311643.3853	4090664.7063	1.55	0.22	67	311674.6041	4090652.9124	1.56	0.22
32	311651.6401	4090695.4202	1.52	0.19	68	311670.1331	4090632.1052	1.62	0.28
33	311657.9141	4090743.9395	2.00	0.14	69	311658.9222	4090561.8639	1.68	0.19
34	311660.3073	4090764.7929	1.13	0.33	70	311650.6886	4090525.4141	1.34	0.23
35	311664.2633	4090782.4663	1.40	0.24	71	311639.3161	4090461.2819	1.72	0.18
36	311668.1960	4090785.7093	1.68	0.19	72	311634.6356	4090431.0436	1.17	0.29

analysis and map creation. All processing was performed in ArcGIS 10.5 software and the ordinary kriging (OK) interpolation was used to generate the contour map, which makes a prediction of the soil penetration resistance and electrical conductivity values in other parts of the test field for sampling. OK, which relies on the spatial correlation of

the data to determine the weighting values, was selected in this study, as the correlation between data points determines the estimated value at an unsampled point. Here we used correlation analysis to detect the spatial correlation between the soil penetration resistance and the electrical conductivity. The correlation analysis result

showed a fairly strong negative correlation in terms of the relationship between the soil penetration resistance and the electrical conductivity (Table 2). As the soil penetration resistance increases, the electrical conductivity decreases. Also, this was the expected result at the beginning of the test.

Three basic certain criteria must be met to use ordinary kriging interpolation technique. First, the data needs to have a normal distribution. Second, the data needs to be stationary. And last, the data cannot have any trends. The histogram of our data includes skewness and kurtosis values (Figure 8). Skewness is a measure of symmetry in distribution. Kurtosis is also a measure of the tails of the distribution. These two statistical values give insights into the shape of the distribution. In a normal distribution, the skewness value should have near 0. If the skewness value is between -0.5 and 0.5, the data are fairly symmetrical and have a normal distribution. Also, the kurtosis value should have near 3. If the kurtosis value is greater than 3, the data have heavier tails than a normal distribution and have leptokurtic distribution. This means that data have a profusion of outliers for normal distribution. If the kurtosis value is less than 3, the data have lighter tails than a normal distribution and have platykurtic distribution. This means that data have a lack of outliers for normal distribution. According to Figure 8, the skewness of the data is 0.08 for soil penetration resistance data. And, the kurtosis value is 1.77 (Figure 8a). The skewness of the data is 0.42 and the kurtosis value is 2.01 for soil electrical conductivity data (Figure 8b). In our study, the results look like it has a fairly good normal distribution for both soil penetration resistance and electrical conductivity data.

In ordinary kriging interpolation, data have to be stationary. If data are stationary, it can be able to obtain meaningful sample statistics such as means, variances, and correlations with other variables. Such statistics are useful as descriptors of future behavior only if the data are stationary. At this point, the entropy Voronoi map presents the local variation of the soil penetration resistance and the electrical conductivity and helps us determine if our data are stationary or not. The entropy Voronoi maps for the soil penetration resistance and the electrical conductivity are shown in Figure 9. In spite of the fact that there is moderate variation in the data as most areas are

light green, yellow, and orange, the entropy Voronoi maps show the data is looking adequately stationary.

The trend analysis that provides a three-dimensional perspective of the data helps identify trends in our dataset across an entire study field (Figure 10). In Figure 10, the green line shows the trend in the east-west direction on the x, z plane and the blue line depicts the trend in the north-south direction on the y, z plane. Generally, we have lower soil penetration resistance values in the center of the east-west direction. However, we have higher soil penetration resistance values in the center of the north-south direction (Figure 10a). On the other hand, we have higher soil electrical conductivity values in the center of the east-west direction. However, we have lower soil electrical conductivity values in the center of the north-south direction (Figure 10b). When both figures are compared, it can be seen that there is a negative relationship between soil physical properties.

The interpolation map is shown in Figure 11. It is observed that the soil penetration resistance values on the left side of the map are lower than the right side when the map is examined visually. Conversely, it is observed that the soil electrical conductivity values on the left side of the map are higher than the right side. This shows that there is a negative relationship between soil penetration resistance and soil electrical conductivity.

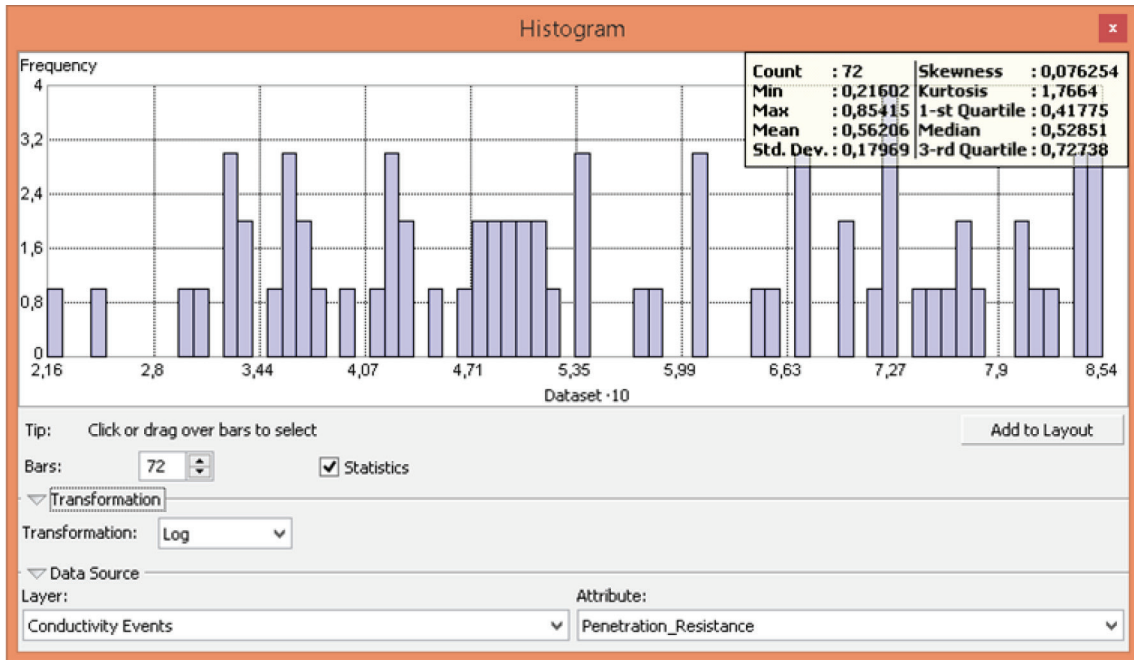
4. Discussion

The field-scale application of soil electrical conductivity measurement has been used to determine a variety of anthropogenic properties: leaching fraction, irrigation and drainage patterns, and compaction patterns due to farm machinery (Corwin et al., 2005). On the other hand, the soil penetration resistance measured by a soil cone penetrometer is the degree of soil compaction. And also, monitoring of the compacted soil through electrical conductivity plays an important role to determine the correlation between soil penetration resistance and the soil electrical conductivity. In the literature, there are not many studies measuring the soil penetration resistance and the soil electrical conductivity by the using mobile combined sensor platform. However, there have been studies to determine the correlation between soil penetration resistance and the soil electrical conductivity.

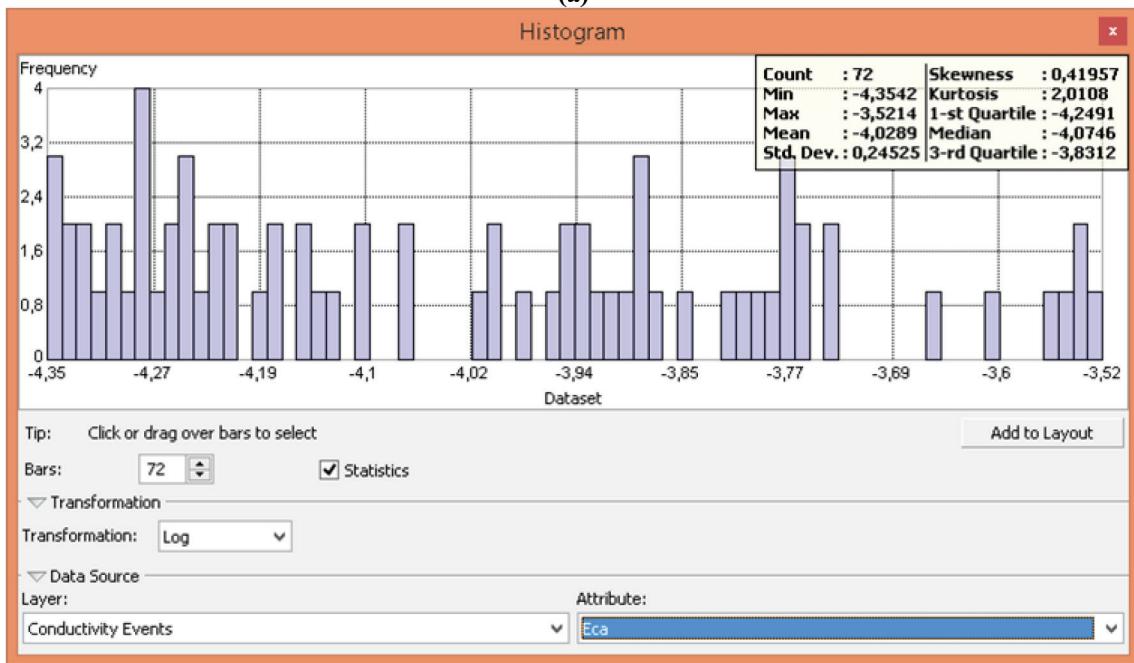
Jabro et al. (2006) determined if Coulter and penetrometer-type EC sensors produce similar descriptions of soil variability, and if EC and PR measured using a penetrometer-type sensor are correlated. Average values of the ECa and PR were measured over a 0 to 30 cm depth. They reported that the soil ECa and CI parameters presented strong to medium spatial dependency and the results indicate the effectiveness of the ECa and CI sensors for identifying spatial variability of soil properties.

Table 2. The correlation analysis relationship between the soil penetration resistance and the electrical conductivity.

	Penetration Resistance	Electrical Conductivity
Penetration Resistance	1	-1.282253
Electrical Conductivity	-0.779877157	1



(a)



(b)

Figure 8. Histograms of normal distribution. a) Soil penetration resistance. b) Soil electrical conductivity (Histogram transformation: Log).

Chen et al. (2009) described the short-term development typically, over the first 3 to 7 days of electrical conductivity and penetration resistance of lime kiln dust modified soils. Researchers used the time-domain reflectometry apparatus to measure the electrical conductivity, and the needle penetrometer test was chosen to measure the

penetration resistance. Researchers reported that the increase in penetration resistance is strongly related to the decrease of the electrical conductivity.

Siqueira et al. (2010) have tried to calculate the correlation between soil resistance penetration and apparent soil electrical conductivity. The studied soil was

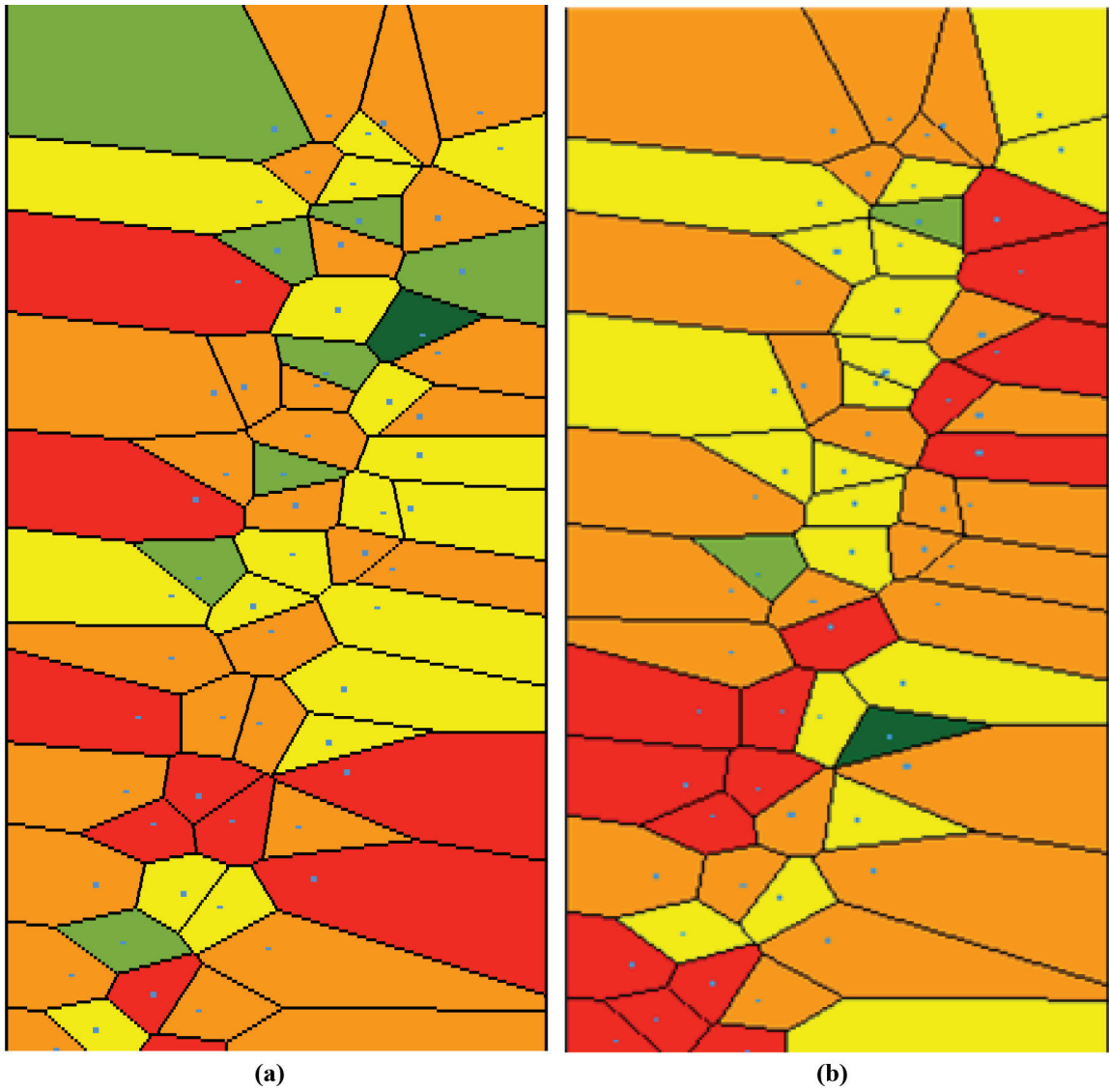


Figure 9. The entropy Voronoi maps. a) Soil penetration resistance. b) Soil electrical conductivity.

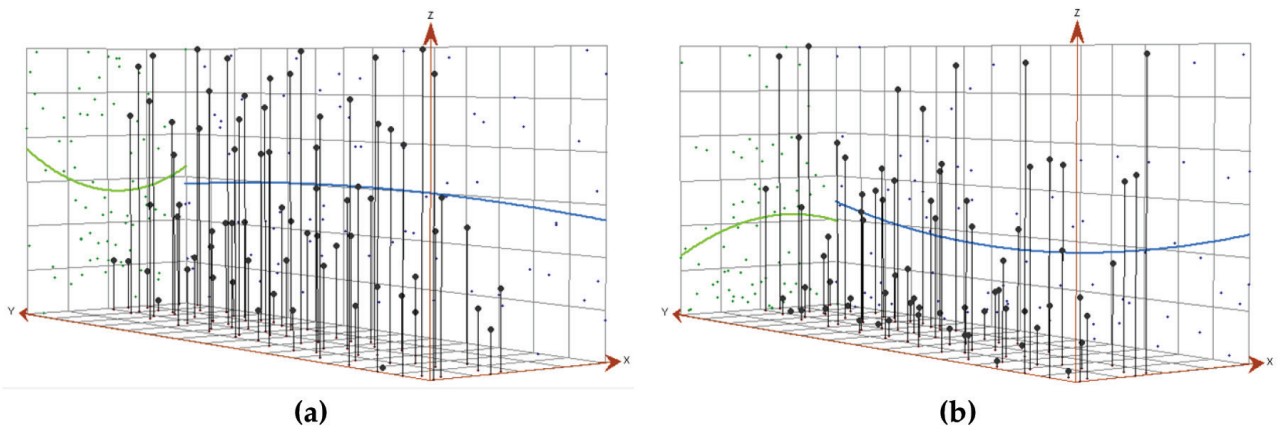


Figure 10. Trend analysis results. a) Trend analysis result of the soil penetration resistance. b) Trend analysis result of the electrical conductivity.

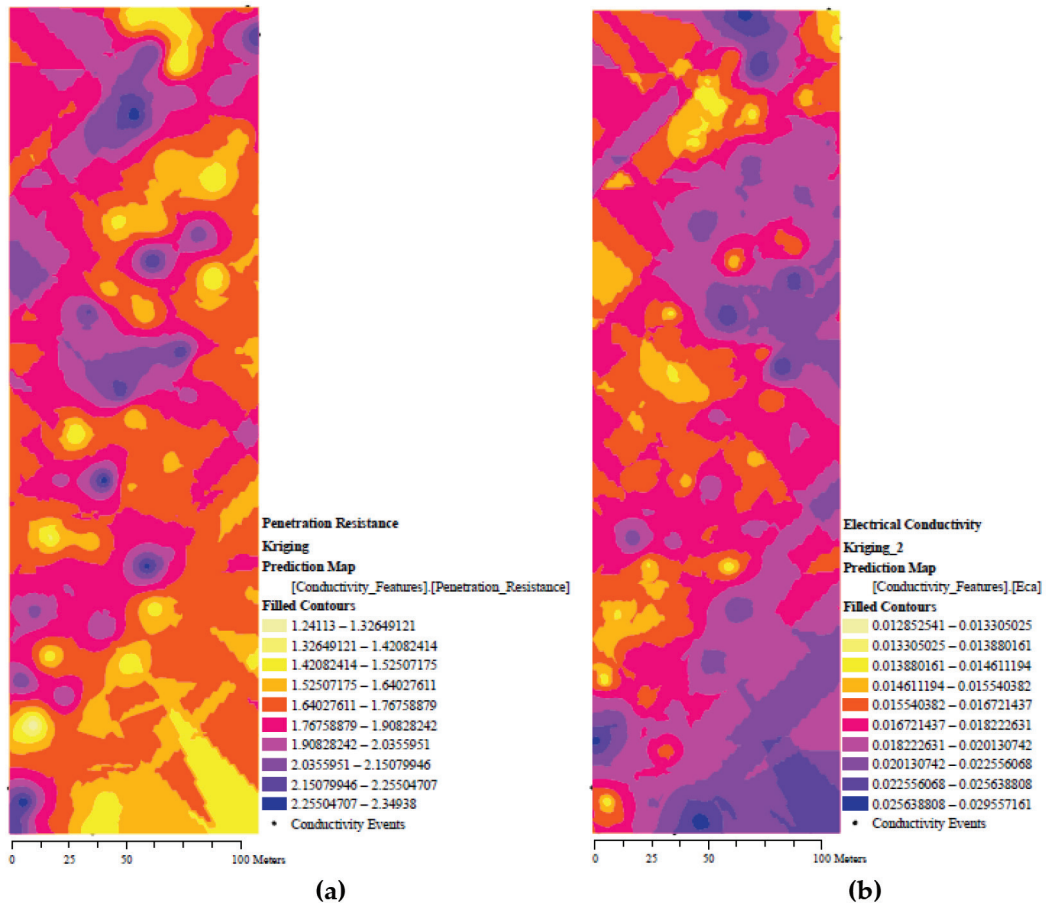


Figure 11. The interpolation maps of the study. a) Map of the soil penetration resistance. b) Map of the soil electrical conductivity.

a gley cambisol. The ECa was measured with EM38DD (Geonics Limited) and the soil resistance penetration was measured with Veris P3000 (Veris Technologies Inc.). Researchers reported that the linear correlation data shown a medium negative correlation between soil resistance penetration and ECa.

Hoefer et al. (2010) evaluated how well nondestructive electrical conductivity measurements localize compacted areas. Researchers measured the penetration resistance with a hand-driven Penetrologger (Eijkelkamp, Giesbeek, The Netherlands). The electromagnetic induction meter (EM38 probe; Geonics, Mississauga, Canada) was used to measure the electrical conductivity of the soil. Researchers reported that the results show a negatively strong correlation between penetration resistance and electrical conductivity, especially in areas with high penetration resistance values.

Siqueira et al. (2014) presented a combined application of an EM38DD for assessing soil apparent electrical conductivity and a dual-sensor vertical penetrometer

Veris P3000 for measuring soil electrical conductivity and soil resistance to penetration. Researchers reported that the electrical conductivity and penetration resistance data show highly significant negative correlation coefficients, once both properties are related to the soil water content.

Bölenius et al. (2018) were conducted a study to determine the correlation of soil penetration resistance, yield, and soil electrical conductivity in east-central Sweden. The researchers reported that study results showed the strong correlations between penetration resistance, electrical conductivity, and yield. They reported that the correlation between yield and penetration resistance was strongest, with $r = -0.67$ and also displayed the strongest correlation between yield and electrical conductivity ($r = 0.48$). It is understood that there is an indirectly negative correlation between penetration resistance and electrical conductivity.

Gülser and Candemir (2012) investigated direct and indirect effects of the some soil properties on penetration resistance in a clay field with organic waste. Researchers

determined some soil properties such as penetration resistance, gravimetric water content, bulk density, relative saturation, mean weight diameter, and total porosity. They reported that the penetration resistance data shown significant negative correlations for total porosity (-0.551), gravimetric water content (-0.439) and mean weight diameter (-0.509), and significant positive correlations for bulk density (0.550) and relative saturation (0.374).

Drummond et al. (2000) reported that, although there is various equipment available to measure the soil penetration resistance and the soil electrical conductivity, the joint measurement of the penetration resistance and the electrical conductivity would allow characterizing the soil not only along the landscape but also in-depth. And also, Pan et al. (2014) reported that the proximal soil measurements that combine soil sensors and data analysis methods to obtain high-resolution soil data of the huge farmland are a useful approaches. In this context, we developed a combined sensor platform for the simultaneous on-the-go measurement of soil penetration resistance and electrical conductivity. The experimental results showed that there was a negatively significant correlation between soil penetration resistance and electrical conductivity like other studies in the literature. No faults were detected in any parts of the system during the field study. The results showed that the developed mobile combined sensor platform is suitable for map-based precision farming studies.

The apparent soil EC values depend on several parameters such as size of the soil, salinity, porosity, and water content. And also, the soil water content varies with depth. In this study, the probe spacings relate to the apparent depth under test, e.g. 50 cm probe spacing. As a result, study data indicates the soil apparent EC at a depth of ~50 cm. The probes only physically penetrate to the soil a few centimetres. However, the volume of geology under test is determined by the spacing between each test

probe. So, in theory, the testable depth is only limited by the instrument's strength of the signal and the deployable distance between probes. So, for each measurement traverse, the probe spacings (between adjacent probes) need to change.

Agricultural soils are significantly affected by physical properties such as bulk density, porosity, water retention capacity, etc. The understanding of the spatial variability of soil physical properties within agricultural fields cannot be possible with measuring only one physical parameter. For this reason, nowadays the researchers show great interest to develop the combined sensor platforms in agricultural studies. In this study, the combined sensor platform that can be mounted on a 4WD agricultural robot was developed to measure the soil penetration resistance and electrical conductivity. Soil penetrometer is the only device that can measure soil strength directly and in situ. But, there are different devices and methods to measure soil electrical conductivity. The Wenner four-probe measurement method was used to measure soil electrical conductivity in this study. The results showed that the developed system has proved to be efficient and capable of measuring the spatial pattern of penetration resistance and electrical conductivity. And also, the soil penetration resistance and the electrical conductivity data were showed a significantly negative correlation. The results of the study show that the developed combined sensor platform can be useful not only for agricultural science but also for other sciences.

Acknowledgment

This work is financially supported by The Scientific Research Projects Coordination Unit of Akdeniz University (project number: FBA-2017-1980). We are very grateful to the Kahramanlar Machine Manufacturing Company and Ms Iveta Puza from Latvia for their cooperation and effort in supporting the experiment.

References

- Alesso CA, Masola MJ, Carrizo ME, Cipriotti PA, del Imhoff S (2019). Spatial variability of short-term effect of tillage on soil penetration resistance. *Archives of Agronomy and Soil Science* 65: 822-832.
- Barnhisel RI, Hower JM (1997). Coal surface mine reclamation in the eastern united states: the revegetation of disturbed lands to hayland/pasture or cropland. *Advances in Agronomy* 61: 233-275.
- Bölenius E, Wetterlind J, Keller T (2018). Can within field yield variation be explained using horizontal penetrometer resistance and electrical conductivity measurements? Results from three Swedish fields. *Acta Agriculturae Scandinavica Section B-Soil And Plant Science* 68: 690-700.
- Chen R, Drnevich VP, Daita RK (2009). Short-term electrical conductivity and strength development of lime kiln dust modified soils. *Journal of Geotechnical and Geoenvironmental Engineering* 135: 590-594.
- Corwin DL, Lesch SM (2005). Apparent soil electrical conductivity measurements in agriculture. *Computers and Electronics in Agriculture* 46: 11-43.
- Drummond PE, Christy CD, Lund, ED (2000). Using an automatic penetrometer and soil ECa probe to characterize the rooting zone. In: *Proceedings of the 5th International Conference on Precision Agriculture*; Bloomington, Minn, USA. pp.

- Feng S, Wen H, Ni S, Wang J, Cai C (2019). Degradation characteristics of soil-quality-related physical and chemical properties affected by collapsing gully: the case of subtropical Hilly Region, China. *Sustainability* 11: 3369.
- Gülser C, Candemir F (2012). Changes in penetration resistance of a clay field with organic waste applications. *Eurasian Journal of Soil Science* 1: 16-21.
- Hoefer G, Bachmann J, Hartge KH (2010). Can the EM38 probe detect spatial patterns of subsoil compaction? In: *Proximal Soil Sensing*, R. (editor). Dordrecht, Netherlands: Springer Science, pp. 265-273.
- Ishaq M, Hassan A, Saeed M, Ibrahim M, Lal R (2001). Subsoil compaction effects on crops in Punjab. Pakistan I. Soil physical properties and crop yield. *Soil and Tillage Research* 59: 57-65.
- Jabro JD, Evans RG, Kim Y, Stevens WB, Iversen WM (2006). Characterization of spatial variability of soil electrical conductivity and cone index using coulter and penetrometer-type sensors. *Soil Science* 171: 627-637.
- Lima RP, Silva AP, Giarola NFB, Silva AR, Rolim MM (2017). Changes in soil compaction indicators in response to agricultural field traffic. *Biosystems Engineering* 162: 110.
- Naderi-Boldaji M, Sharifi A, Jamshidi B, Younesi-Alamouti M, Minaee, S (2011). A dielectric-based combined horizontal sensor for on-the-go measurement of soil water content and mechanical resistance. *Sensors and Actuators A Physical* 171: 131-137.
- Nawaz MF, Bourrie G, Trolard F (2013). Soil compaction impact and modelling. A review. *Agronomy for Sustainable Development* 33: 291.
- Pan L, Adamchuk VI, Prasher S, Gebbers R, Taylor RS, Dabas M (2014). Vertical Soil Profiling Using a Galvanic Contact Resistivity Scanning Approach. *Sensors* 14: 13243-13255.
- Servadio P, Bergonzoli S, Beni C (2016). Soil Tillage Systems and Wheat Yield under Climate Change Scenarios. *Agronomy* 6: 43.
- Siqueira GM, Dafonte JD, Lema JB, Paz Gonzalez A (2010). Correlation between soil resistance penetration and soil electrical conductivity using soil sampling schemes. *Proceedings 19th World Congress of Soil Science*, 1-6 August, Brisbane, Australia.
- Siqueira GM, Dafonte JD, Lema JB, Armesto MV, Silva, EF (2014). Using Soil Apparent Electrical Conductivity to Optimize Sampling of Soil Penetration Resistance and to Improve the Estimations of Spatial Patterns of Soil Compaction. *The Scientific World Journal* 2014: 1-12.
- Ünal İ, Kabaş Ö, Sözer S (2020). Real-Time Electrical Resistivity Measurement and Mapping Platform of the Soils with an Autonomous Robot for Precision Farming Applications. *Sensors* 20: 251.
- Valera DL, Gil J, Agüera J (2012). Design of a New Sensor for Determination of the Effects of Tractor Field Usage in Southern Spain: Soil Sinkage and Alterations in the Cone Index and Dry Bulk Density. *Sensors* 12: 13480-13490.
- Valjaots E, Lehiste H, Kiik M, Leemet T (2018). Soil sampling automation using mobile robotic platform. *Agronomy Research* 16: 917-922.
- Verified Market Research (2018). VMR [Online]. Global Agriculture Robots Market Size By Type (Driverless Tractors, Automated Harvesting Machine, Others), By Application (Field Farming, Dairy Management, Indoor Farming, Others) By Geography Scope and Forecast. Website <https://www.verifiedmarketresearch.com/product/global-agriculture-robots-market-size-and-forecast-to-2025/> [accessed 13 January 2021].
- Zeng Q, Sun Y, Lammers PS, Ma D, Lin J, Hueging H (2008). Improvement of a dual-sensor horizontal penetrometer by incorporating an EC sensor. *Computers and Electronics in Agriculture* 64: 333-337.